

Cold melting and solid structures of dense lithium

Christophe L. Guillaume¹, Eugene Gregoryanz^{1*}, Olga Degtyareva¹, Malcolm I. McMahon¹, Michael Hanfland^{2*}, Shaun Evans², Malcolm Guthrie³, Stanislav V. Sinogeikin⁴ and H-K. Mao^{3,4}

Recent theoretical and experimental studies have produced several unusual and interesting results on dense lithium, the first metal in the periodic table. These include the deviation from simple metal behaviour, superconductivity at 17 K, and a metal to semiconductor transition^{1–5}. Despite these efforts, at present there is no agreement on the location of the high-pressure solid phases and melting curve of Li, and there is no clear picture of its phase diagram above 50 GPa (refs 4–7). Using powder and single-crystal high-pressure diffraction techniques, we have mapped out the lithium phase diagram up to 130 GPa over a wide temperature range between 77 and 300 K. Whereas the melting temperatures of materials usually rise under pressure, and even the lightest condensed gases, hydrogen and helium, melt at temperatures of the order of 10^3 K at 50 GPa (refs 8,9), we find that at these pressures lithium remains a liquid at temperatures as low as 190 K, by far the lowest melting temperature observed for any material at such pressure. We also find that in its solid state above 60 GPa, lithium adopts three novel and complex crystal structures not previously observed in any element. Estimates of the zero-point energy suggest that quantum effects play a significant role in shaping the lithium phase diagram.

The familiar properties and states of matter can be markedly modified by applying pressure and temperature. Besides those encountered in daily life (gas, liquid and solid), some exotic states, for example superfluids or superconductors, can be observed. Quantum effects, the energies of which are very small on an everyday scale, are responsible for the formation of these unusual forms of matter. To create any of these states, low temperatures are needed to decrease the energy of the system to the level where the quantum effects become dominant. Conversely, by applying pressure, and thereby bringing the atoms closer to each other, it is possible to increase the kinetic energy (that is, the zero-point energy) of the system. If the other energy terms that make up the total energy increase more slowly with pressure than the zero-point energy, it might be possible to reach a compression at which the quantum effects play the dominant role¹⁰. One of the obvious consequences of the zero-point energy being comparable to or in excess of differences in characteristic structural energies per atom would be melting of the solid under compression (cold melting)^{10,11}. For light elements, such as hydrogen, melting influenced by the zero-point energy is expected to happen even at $T = 0$ (at compressions which are at present beyond the capabilities of experimental techniques), leading to a metallic liquid ground state with exotic properties¹².

Is it then possible to create a metallic liquid ground state in systems other than dense hydrogen? Most metallic elements with strong interatomic interactions are solids under normal conditions,

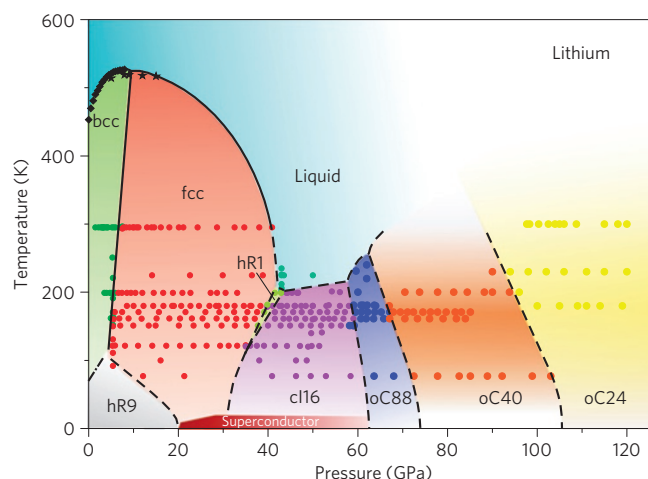


Figure 1 | Proposed phase diagram of lithium over a wide pressure-temperature range. Apart from bcc and fcc, the phases are labelled with their structural types using the Pearson notation. The solid coloured symbols show some of the P - T points covered in this study. The errors on pressure and temperature measurements are ± 2 GPa and ± 10 K respectively. The filled black diamonds and stars are from refs 6 and 30. The location of the hR9 phase is adapted from ref. 31. The superconducting region is drawn to combine all experimental points from refs 3, 16–18.

with melting temperatures $T_m \sim 10^3$ K resulting from their high cohesive energies (1–10 eV/atom). There is one exception, mercury (Hg), which is a liquid metal at 1 atm, with $T_m = 234$ K, and a superconductor, with $T_c = 4.2$ K. Mercury has a lower cohesive energy than most metals, but its large atomic mass prevents the zero-point energy from playing any significant role, and its melting temperature rises quickly under pressure¹³, a normal behaviour for most materials on compression. At low compressions ($P \leq 10$ GPa) only a few metallic elements are known to show a negative slope of the melting curves, over a very narrow pressure range of ~ 1 GPa (for example, Ga, Bi, Cs; ref. 13). Recently, an unprecedented decrease in the melting temperature of sodium, from 1,000 to 300 K, over a pressure range of ~ 90 GPa was discovered experimentally¹⁴. It was suggested that the large number of well-defined low-symmetry crystalline phases observed around the melting minimum might be the result of a relatively flat energy landscape having several shallow minima, the occupation of which could be influenced by the increased energy of quantum effects¹⁵.

An obvious lighter-mass candidate, where the quantum effects might play a greater role, is lithium. There are some similarities between sodium and lithium—both are nearly free-electron metals

¹SUPA, School of Physics and Astronomy, and Centre for Science at Extreme Conditions, The University of Edinburgh, Edinburgh, EH9 3JZ, UK, ²ESRF, BP 220, Grenoble, France, ³Geophysical Laboratory, Carnegie Institution of Washington, Washington DC 20015, USA, ⁴HPCAT, Carnegie Institution of Washington, Argonne, Illinois 60439, USA. *e-mail: e.gregoryanz@ed.ac.uk; hanfland@esrf.fr.

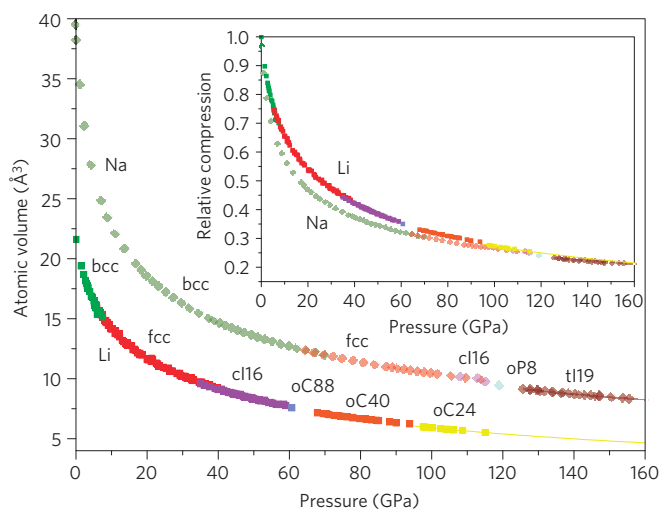


Figure 2 | Equations of state of lithium and sodium. Equations of state of Li and Na measured in this and the previous study (ref. 15). Inset: Relative compression of both metals. Different colours of the solid symbols represent different crystallographic phases, as described in the text and in ref. 15.

at normal pressure, crystallizing in a body-centred cubic (bcc) structure at room temperature. On compression, both first transform to a face-centred cubic (fcc) structure and later exhibit the same pressure-induced symmetry lowering^{2,15}. Very recently, using a multi-anvil cell technique, the melting temperature of Li was measured up to 15 GPa, with results suggesting a maximum followed by a negative slope of the melting curve⁶, similar to that observed in Na (ref. 14). Nevertheless, the electronic properties of Li appear to deviate significantly from those of Na. Unlike sodium, lithium becomes superconducting at 0.4 mK both at ambient pressure¹⁶ and above 20 GPa (refs 3,17,18). The dependence of T_c in Li between ambient pressure and 20 GPa is not known, but above 20 GPa (see Fig. 1) the superconducting temperature increases dramatically, reaching ~ 17 K at around 50–60 GPa—one of the highest values known among the elements^{3,17,18}. Experimental difficulties associated with the static compression of lithium have

hindered experimental efforts in studying its dense states (see also the Methods section). At the same time, lithium, being the metal with the lowest atomic number, has attracted considerable theoretical interest. Recent years have seen a slew of theoretical papers analysing the structural, electronic, superconducting and melting properties of Li over a wide pressure–temperature range (see refs 1,4,19–24 and references therein). However, there is no agreement between the theoretical and experimental studies on the Li phase diagram at pressures above 50 GPa (for example refs 4–7,24 on the location of the solid phases and the melting temperatures). More importantly, there is no clear picture of the physical properties and states of dense lithium over a wide pressure and temperature range.

To investigate the behaviour of dense lithium, we have mapped out its phase diagram over a wide P – T range by means of powder and single-crystal X-ray synchrotron diffraction (see the Methods section for the experimental details). The results summarizing the behaviour of the solid phases and melting curve discovered in this study are shown in Fig. 1. Our location of the Li melting curve reveals a dramatic drop in the melting temperature. Between 40 and 60 GPa (where the density is 2–2.5 times that found at ambient pressure, see Fig. 2) lithium melts at around 190 K, the lowest melting temperature among the elemental metals. More interestingly, in the pressure range where the melting curve reaches its minimum, lithium is a superconductor with $T_c = 17$ K. At this point the liquid and superconducting state are separated by only $\Delta T \sim 175$ K—the smallest known ΔT in any system. Our data show that at pressures above 60 GPa the melting curve recovers its positive slope and starts to rise again. This pressure corresponds to a structural change in the solid state. We find that the stability range of the previously known highest-pressure c16 phase² extends from ~ 45 to 60 GPa at temperatures below 200 K. On further compression, the c16 structure transforms into an orthorhombic C-face centred phase having 88 atoms per unit cell, oC88, with $a = 8.569(6)$ Å, $b = 9.282(8)$ Å, $c = 8.389(4)$ Å and unit cell volume of $V = 667.1(1)$ Å³ at 61(2) GPa, see Fig. 3a. (See Fig. 2 for the equation of state of all phases and the Methods section for information on the number of atoms.) The visual appearance of the sample clearly changes at the c16 to oC88 transition, from relatively shiny in the fcc and c16 phases to grey (insets to Fig. 3 show representative microphotographs of the same sample

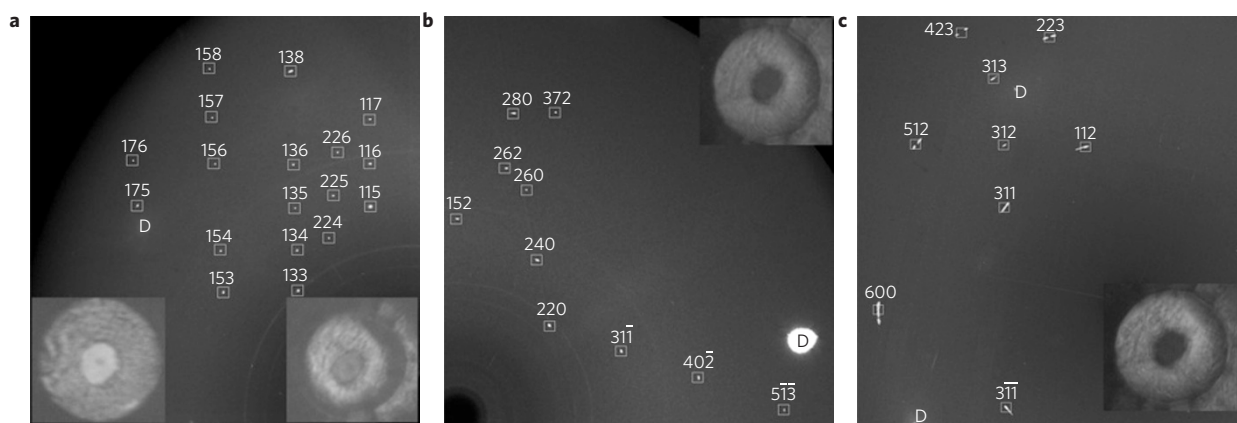


Figure 3 | Composite diffraction images from the oC88, oC40 and oC24 phases. **a**, Diffraction data from the oC88 phase at 65 GPa and 180 K collected over a 13° scan range. The left inset shows the visual appearance of the sample in the c16 phase at 45 GPa and 180 K. The right inset shows the same sample in the oC88 phase at 65 GPa and 180 K. **b**, Diffraction data from the oC40 phase of Li at 90 GPa and 180 K collected over a 25° scan range. The inset shows the sample appearance of this phase at 90 GPa and 180 K. **c**, Diffraction data from the oC24 phase of Li at 125 GPa and 300 K collected over a 23° scan range. The inset shows the sample appearance in the oC24 phase at 130 GPa and 300 K. In all images, squares mark lithium reflections and are labelled by their hkl indices. A reflection from the diamond is marked by the letter 'D' and the visible powder rings are from the rhenium gasket. Other small diffraction spots are of a different appearance from those indexed and do not emanate from the lithium sample. The diameter of the sample is ~ 50 μm in all cases.

at different pressures). The oC88 phase has only a narrow pressure stability range, and at ~ 70 GPa at 150 K it transforms to another C-face centred orthorhombic structure having 40 atoms per unit cell (oC40) (see Fig. 3b) with $a = 4.815(4)$ Å, $b = 7.948(9)$ Å, $c = 6.613(2)$ Å and $V = 253.1(4)$ Å³ at 90(2) GPa. The oC40 phase has a wider stability range than oC88, extending to above 100 GPa at 77 K. Visually, the sample becomes still darker at the oC88 to oC40 transition, which correlates with the recently reported pressure of the metal-to-semimetal transition⁵. If oC40 is compressed further it transforms to a third C-faced centred orthorhombic phase with 24 atoms per unit cell (oC24) (see Fig. 3c) with $a = 4.213(2)$, $b = 7.482(7)$, $c = 4.205(2)$ and $V = 132.5(7)$ Å³ at 115(2) GPa. This phase seems to be stable to at least 130 GPa, the highest pressure reached in this study. Our visual observations of all three solid phases are consistent with electrical conductivity measurements⁵ which observed a dramatic increase in resistivity with pressure, although it seems that the oC24 phase most probably was not reached in that study (compare our Fig. 1 and Fig. 2 in ref. 5). The large number of atoms (88 and 40) involved in the lower-pressure phases would make any theoretical predictions and energy calculations a formidable task. As a result, to the best of our knowledge, neither the oC88 phase nor the oC40 phase has ever been considered as thermodynamically stable between 50 and 100 GPa in previous calculations, whereas several structures with 24 atoms having low, and sometimes competing, enthalpies have been proposed^{19,22–24}. Our diffraction data of the highest pressure phase confirm the oC24 (Cmca-24) structure originally proposed by Rousseau *et al.*¹⁹ (the refinement of the structures and other details of the solid phases described here will be published separately).

The important question which arises from our observations is why does the melting temperature of lithium decrease so much under pressure? The stability of the metallic lattice is determined by competing energy terms, such as the kinetic energy of the electrons and the Coulomb energy (which in turn consists of several different terms). As these energy terms depend differently on volume, and compete with each other as the volume is reduced, pressure can change the balance in favour of the electronic band-structure energy contribution¹⁰. The sum of all energy terms competing differently as volume is reduced could result in a minimum in the electronic density of states, leading to an energy gap, a so-called Peierls distortion, which was previously shown to be responsible for the lowering of the crystal structure symmetry in Li and the appearance of the cI16 structure². It was argued that for lithium the same mechanism creates an energy gap at the Fermi energy level in the liquid, thus lowering the electronic (and total) energy and making the liquid energetically preferred to a crystalline state⁴.

The same theoretical study that investigated the melting curve and molten states of Li also tried to establish the existence of low-symmetry solid structures⁴. Our study reveals a sequence of low-symmetry structures that were not predicted and melting temperatures as much as 50% lower than those previously calculated. One of the possible explanations for the discrepancies (particularly in the melting temperature) between theory and experiment is the zero-point energy and the influence of quantum effects which were not considered in the theoretical studies. Using the phonon density of states it is possible to calculate the ground-state energy of a system, and therefore the zero-point energy²⁵, but such calculations are beyond the scope of this study. However, one can estimate the zero-point energy using a Raman mode, particularly if it represents the high-end frequency of the phonon spectrum. The bcc and fcc phases of Li and Na do not have first-order Raman bands, whereas our Raman studies on the cI16 phases of both metals show Raman activity with the characteristic wavelengths of ~ 70 cm⁻¹ for Na at 115 GPa and 150–180 cm⁻¹ for Li between 40 and 60 GPa. This measurement would give underestimated Debye temperatures

(and zero-point energies²⁶) on the order of 200 K for Li at 50 GPa and 110–120 K for Na at 120 GPa (the estimation for Na is in rather good agreement with the calculated Debye temperature²⁷). This crude estimation implies that in Li at 50 GPa the zero-point energy is comparable to its melting temperature, and that quantum dynamics plays a significant role in shaping the lithium phase diagram.

Our study raises the intriguing question of whether it is possible to ‘construct’ a system, other than pure hydrogen, possessing a metallic liquid ground state. At present there are no experimentally known liquid metallic ground states, and if such states do exist their properties will most probably be highly unusual, as predicted for hydrogen¹². To create such a state two conditions need to be fulfilled: light masses of the constituent materials and weak attractive interactions. It is interesting to note that at present the only other metallic compound with a lower (at atmospheric pressure) melting temperature than that described in this study is the lithium-rich compound lithium tetraammine Li(NH₃)₄ (ref. 28), where $T_m = 88$ K. As its mass ‘per atom’ is even lower than that of lithium, and the attractive forces are probably not purely electrostatic, it satisfies both of the criteria outlined above. It might then be possible that by tuning its electronic properties by pressure, or by further doping, one could achieve a previously unobserved novel state of matter.

Methods

We have conducted 35 independent experiments, varying in pressures from 5 to 130 GPa at temperatures from 77 to 300 K. We have used symmetric membrane-driven diamond anvil cells equipped with diamonds of different sizes and Re or Ir gaskets indented to between 6 and 15 μm to confine the sample. The angular openings of our cryostat and pressure cells allowed data to be collected to 50° in 2θ. The pressure was determined from the diffraction pattern of a small grain (1–2 μm) of Ta placed in the sample chamber together with the lithium, and was also correlated with the diamond Raman edge shift and/or with the pressure determined from the diffraction pattern of the gasket material. Diffraction data were collected on the high-pressure beamline ID-09 at the European Synchrotron Radiation Facility (ESRF) and beamline 16-ID-B (HPCAT) at the Advanced Photon Source. Monochromatic X-ray beams with wavelengths of around ~ 0.4 Å were used, and the diffraction data were recorded on a MAR CCD or MAR555 detector, placed 150–300 mm from the sample.

There are several problems with the confinement of lithium in diamond anvil cells at high pressures, including pressure-induced chemical reaction with diamonds at temperatures above 200 K, and penetration of the small Li atoms into optically undetectable cracks on the surface of the diamond. In both cases, this leads to an abrupt change of the sample appearance; the loss of pressure and the sample; a change in the diffraction pattern; and typical diamond damage (see also ref. 29). We have tried several methods (including the use of pressure transmitting media) to prevent the chemical reaction and/or penetration of Li atoms into diamond. We found that using the smallest possible sample chamber (and thus the smallest area of contact between the Li and diamond) and low temperatures (<200 K) can significantly reduce the disintegration of the diamonds at high pressures. However, in some cases we were able to collect data between 200 and 300 K for short periods of time (2–3 h). At temperatures below 200 K we never observed lithium-related damage, even with the sample in the liquid state. We have followed numerous P – T paths with decreasing/increasing pressure and temperature to confirm both the identity and reproducibility of the crystalline phases on compression and on cooling from the melt, and to rule out the chemical reaction of the sample.

As a result of the low atomic number of lithium and the thickness of the sample (which we estimated as varying between 3 and 8 μm at different pressures) it was not possible to observe the diffraction signal from the liquid state. However, we were able to detect melting from the disappearance of the crystalline diffraction pattern on changing P – T conditions, for example temperature increase/decrease when in the cI16 phase or pressure increase/decrease when in the fcc/oC88 phases, and its reappearance when the change was reversed. The large apertures of the cells and cryostat allowed us to cover a sufficiently large portion of reciprocal space to distinguish melting from the appearance of solid phases with a very limited number of reflections, for example, bcc or fcc observed at different P – T conditions. We have also observed melting visually when the melting line was crossed, consistent with the simultaneous disappearance of the diffraction pattern.

The number of atoms per unit cell for the oC88 structure was estimated from the assumption of continuity of atomic volume through the cI16 → oC88 phase transition. The same assumption was applied when estimating the number of atoms for the oC40 and oC24 phases. At 59 GPa, just before the transformation to

the oC88 phase, the atomic volume of the cI16 phase is $7.750(1) \text{ \AA}^3$. All possible space groups for the oC88 phase required the number of atoms per unit cell to be a multiple of four, leaving 88 as the most plausible number giving less than a 0.5% volume discontinuity at the phase transition. In the cases of the oC40 and oC24 phases, the similar constraints imposed by the space groups and volume continuity yielded 40 and 24 atoms respectively. For the oC24 phase, two other possible numbers are 20 or 28, but these give an unrealistic volume difference at the oC40 to oC24 transition, thus constraining the equation of state above 100 GPa.

Received 14 May 2010; accepted 26 October 2010;
published online 9 January 2011

References

- Neaton, J. B. & Ashcroft, N. W. Pairing in dense lithium. *Nature* **400**, 141–144 (1999).
- Hanfland, M., Syassen, K., Christensen, N. E. & Novikov, D. L. New high-pressure phases of lithium. *Nature* **408**, 174–178 (2000).
- Shimizu, K., Ishikawa, H., Takao, D., Yagi, T. & Amaya, K. Superconductivity in compressed lithium at 20 K. *Nature* **419**, 597–599 (2002).
- Tamblyn, I., Raty, J. & Bonev, S. Tetrahedral clustering in molten lithium under pressure. *Phys. Rev. Lett.* **101**, 075703 (2008).
- Matsuoka, T. & Shimizu, K. Direct observation of a pressure-induced metal-to-semiconductor transition in lithium. *Nature* **458**, 186–189 (2009).
- Lazicki, A., Fei, Y. & Hemley, R. High pressure differential thermal analysis measurements of the melting curve of lithium. *Solid State Commun.* **150**, 625–627 (2010).
- Hernández, E., Rodríguez-Prieto, A., Bergara, A. & Alfé, D. First-principles simulations of lithium melting: Stability of the bcc phase close to melting. *Phys. Rev. Lett.* **104**, 185701 (2010).
- Datchi, F., Loubeyre, P. & LeToullec, R. Extended and accurate determination of the melting curves of argon, helium, ice (H₂O), and hydrogen (H₂). *Phys. Rev. B* **61**, 6535–6546 (2000).
- Gregoryanz, E., Goncharov, A. F., Matsuishi, K., Mao, H. K. & Hemley, R. J. Raman spectroscopy of hot dense hydrogen. *Phys. Rev. Lett.* **90**, 175701 (2003).
- Abrikosov, A. Some properties of strongly compressed matter. *Sov. Phys. JETP* **12**, 1254–1259 (1961).
- Kirzhnits, D. Internal structure of super-dense stars. *Sov. Phys. JETP* **11**, 365–368 (1960).
- Babaev, E., Sudbø, A. & Ashcroft, N. W. A superconductor to superfluid phase transition in liquid metallic hydrogen. *Nature* **431**, 666–668 (2004).
- Tonkov, E. & Ponyatovsky, E. *Phase Transformations of Elements under High Pressure* (CRC Press, 2005).
- Gregoryanz, E. *et al.* Melting of dense sodium. *Phys. Rev. Lett.* **94**, 185502 (2005).
- Gregoryanz, E. *et al.* Structural diversity of sodium. *Science* **320**, 1054–1057 (2008).
- Tuoriniemi, J. *et al.* Superconductivity in lithium below 0.4 mK at ambient pressure. *Nature* **447**, 187–189 (2007).
- Struzhkin, V. V. *et al.* Superconductivity in dense lithium. *Science* **298**, 1213–1215 (2002).
- Deemyad, S. & Schilling, J. S. Superconducting phase diagram of Li metal in nearly hydrostatic pressures up to 67 GPa. *Phys. Rev. Lett.* **91**, 167001 (2003).
- Rousseau, R., Uehara, K., Klug, D. D. & Tse, J. S. Phase stability and broken-symmetry transition of elemental lithium up to 140 GPa. *ChemPhysChem* **6**, 1703–1706 (2005).
- Rodríguez-Prieto, A. & Bergara, A. Pressure induced complexity in a lithium monolayer: *Ab initio* calculations. *Phys. Rev. B* **72**, 125406 (2005).
- Kasinathan, D. *et al.* Superconductivity and lattice instability in compressed lithium from Fermi surface hot spots. *Phys. Rev. Lett.* **96**, 047004 (2006).
- Ma, Y., Oganov, A. & Xie, Y. High-pressure structures of lithium, potassium, and rubidium predicted by an *ab initio* evolutionary algorithm. *Phys. Rev. B* **78**, 014102 (2008).
- Pickard, C. & Needs, R. Dense low-coordination phases of lithium. *Phys. Rev. Lett.* **102**, 146401 (2009).
- Yao, Y., Tse, J. & Klug, D. Structures of insulating phases of dense lithium. *Phys. Rev. Lett.* **102**, 115503 (2009).
- Wallace, D. Evaluation of thermodynamic functions of elemental crystals and liquids. *Phys. Rev. E* **56**, 1981–1986 (1997).
- Carrera, A. *et al.* First-principles multiphase equation of state of carbon under extreme conditions. *Phys. Rev. B* **78**, 024101 (2008).
- Martínez-Canales, M. & Bergara, A. Lindemann criterion and the anomalous melting curve of sodium. *J. Phys. Chem. Solids* **69**, 2151–2154 (2008).
- Zurek, E., Edwards, P. & Hoffman, R. A molecular perspective on lithium-ammonia solutions. *Angew. Chem.* **48**, 8198–8232 (2009).
- Hanfland, M., Loa, I., Syassen, K., Schwarz, U. & Takemura, K. Equation of state of lithium to 21 GPa. *Solid State Commun.* **112**, 123–127 (1999).
- Luedemann, H. & Kennedy, G. Melting curves of lithium, sodium, potassium and rubidium to 80 kilobars. *J. Geophys. Res.* **73**, 2795–2805 (1968).
- Vaks, V. *et al.* An experimental and theoretical study of martensitic phase transitions in Li and Na under pressure. *J. Phys. Condens. Matter* **1**, 5319–5335 (1989).

Acknowledgements

The authors are grateful to N. Ashcroft, A. Bergara and S. Bonev for very useful discussions. This work is supported by a research grant from the UK Engineering and Physical Sciences Research Council and facilities made available by the European Synchrotron Radiation Facility. Some of the single-crystal data were collected under ESRF LTP project HS-3090. APS is supported by DOE-BES, under Contract No. DE-AC02-06CH11357. HPCAT is supported by DOE-BES, DOE-NNSA and NSF. Work carried out at HPCAT was supported as part of the EFree initiative, funded by the US Department of Energy, Office of Science, under Award Number DE-SC0001057. O.D. acknowledges support from the Royal Society.

Author contributions

C.L.G. conceived and designed the experiments, carried out the experiments and contributed materials/analysis tools. E.G. conceived and designed the experiments, carried out the experiments, analysed the data, contributed materials/analysis tools and wrote the paper. O.D. analysed the data, contributed materials/analysis tools and wrote the paper. M.I.M. analysed the data, contributed materials/analysis tools, carried out the experiments and wrote the paper. M.H. conceived and designed the experiments, carried out the experiments, analysed the data, contributed materials/analysis tools. S.E., S.V.S. and M.G. contributed materials/analysis tools and carried out the experiments. H-K.M. contributed materials/analysis tools.

Additional information

The authors declare no competing financial interests. Reprints and permissions information is available online at <http://np.nature.com/reprintsandpermissions>. Correspondence and requests for materials should be addressed to E.G. or M.H.